# SOME RECENT PROBLEMS OF NUCLEAR THERMODYNAMICS*

K. GROTOWSKI

M. Smoluchowski Institute of Physics, Jagellonian University
Reymonta 4, 30-059 Kraków, Poland
and H. Niewodniczański Institute of Nuclear Physics, Cracow

*(Received December 9, 1999)*

The thermodynamic (statistical) description of the atomic nucleus works well at low excitation energies. Difficulties appear at higher excitations, where phase transitions are expected.

PACS numbers: 25.70.Gh, 25.70.Lm, 25.70.Pq

In my talk I will discuss certain problems of nuclear thermodynamics at medium energies, where sub-nucleonic degrees of freedom may be neglected. Thermodynamics has been used in nuclear physics since the early days. The concept of nuclear temperature, $T$, was introduced by Weisskopf, Landau and Frenkel more than sixty years ago [1]. For an equilibrated system (atomic nucleus):

$$T^{-1} = \frac{\partial S}{\partial E}\,, \tag{1}$$

where entropy $S$ can be calculated from the density of nuclear states, $\rho_{\rm st}$:

$$S = \ln \rho_{\rm st}(E)\,. \tag{2}$$

To be quite accurate, one should take for $\rho_{\rm st}(E)$ the number of states in the energy range equal to the square root of the mean square value of the energy fluctuation [2]. In the Fermi gas approximation (no spin) :

$$\rho_{\rm st}(E) \sim \exp\left[2(aE)^{1/2}\right]\,. \tag{3}$$

* Invited talk presented at the XXVI Mazurian Lakes School of Physics, Krzyże, Poland, September 1–11, 1999.

For a moderate excitation energy, $E$, below about 1 MeV/nucleon, one has $a \approx A/8$ MeV$^{-1}$ [3]. The temperature of a nuclear droplet is now:

$$T \approx \sqrt{\frac{8E}{A}}\,[\mathrm{MeV}]\,, \tag{4}$$

and roughly $T \approx \langle E/n \rangle$, where $n$ denotes the number of excited nucleons [4]. In fact $\rho_{\mathrm{st}}$ also depends on the shell, on pairing effects and slightly on the excitation energy.

The thermodynamic (statistical) description of the atomic nucleus works remarkably well. See, for example the sequential evaporation spectra of $^{1}$H and $^{4}$He particles from the $^{19}$F+$^{64}$Ni reaction at 120 MeV [5] (Fig. 1). In the logarithmic plot, the nuclear temperature is given by the slope of the

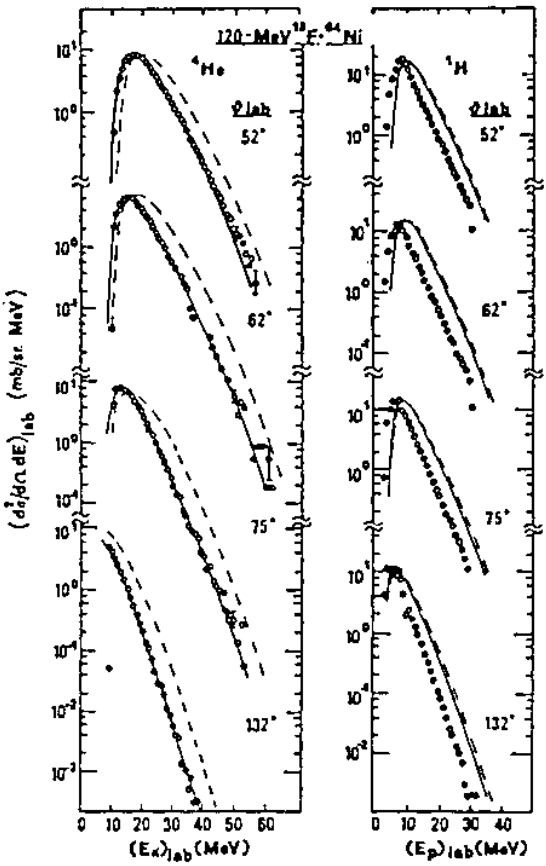


Fig. 1. Energy spectra of protons and alpha particles emitted from the hot $^{83}$Rb nucleus excited to the energy 103 MeV.

energy distribution. Using the sequential particle evaporation picture based on the models of Bohr [6] and Weisskopf [7] one should keep in mind that, besides the statistical equilibrium of the nucleus before and after each emission of a fragment, the second assumption of Weisskopf is important. Each emission should be independent of the previous one, in the sense that the particle emission time, $\tau_{\text{emission}}$, is long in comparison to the characteristic time-scale of variations of the Coulomb barrier caused by the previously emitted fragment. This characteristic time-scale, $\tau_{\text{Coul}}$, is on the order of $10^{-21}$ sec [8].

The situation is not so simple at higher excitation energies up to 10 MeV/nucleon. Can these nuclei still behave as thermally equilibrated systems? This is a controversial problem. Hot nuclei are produced in nuclear collisions. The shape relaxation time of the created system (*e.g.* of the electric quadrupole moment) is on the order of $10^{-23}$ sec, while the nucleon emission time varies from about $10^{-18}$sec at $T = 1$ MeV down to about $10^{-22}$ sec at $T = 5$ MeV [9]. An optimist might say that we are on the safe side, as long as $\tau_{\text{relaxation}} < \tau_{\text{emission}}$.

A pessimist might additionally ask if one can apply thermodynamics and statistical physics for such small systems as atomic nuclei. But the corresponding number of microstates is not so small, *e.g.* for $^{131}$Xe at $T \approx 5$ MeV the entropy $S = \ln n_{\text{st}} \approx 75$ and $n_{\text{st}} \approx 10^{25}$ [10].

## 1. First order phase transition in a macroscopic fluid

For a macroscopic fluid, evaporation of atoms (molecules) by a liquid or condensation of a vapor is under certain conditions described as the first order liquid–vapor (vapor–liquid) phase transition. It proceeds through metastable states and is a stochastic process. Fig. 2 presents the location of the metastable regions on the van der Waals isotherm. Here AD and EB delimits the vapor and the liquid metastable region, respectively. Let us assume a homogenous vapor transferred to some point $X$ of the metastable region. Due to chaotic collisions a cluster (droplet) of $n$ molecules may appear in the vapor. This may immediately decay or survive depending upon its size, $n$, and the work, $W_n$, necessary for its creation [11].

$$W_n = (\mu_l - \mu_\nu)n + 4\pi r^2\sigma = (\mu_l - \mu_\nu)n + \alpha n^{2/3}\,. \tag{5}$$

Here $\mu_l$ and $\mu_\nu$ denotes the liquid and vapor chemical potential, respectively, $r$ is the cluster radius and $\sigma$ the surface tension. The proportionality coefficient $\alpha$ is positive. In the undersaturated vapor (*e.g.* at point $F$) $(\mu_l - \mu_\nu) > 0$, $W_n$ increases monotonously with $n$ and consequently there is no spontaneous condensation of the vapor. At point $X$, in the supersaturated vapor, $(\mu_l - \mu_\nu) < 0$ and $W_n$ reaches a maximum, and then goes to

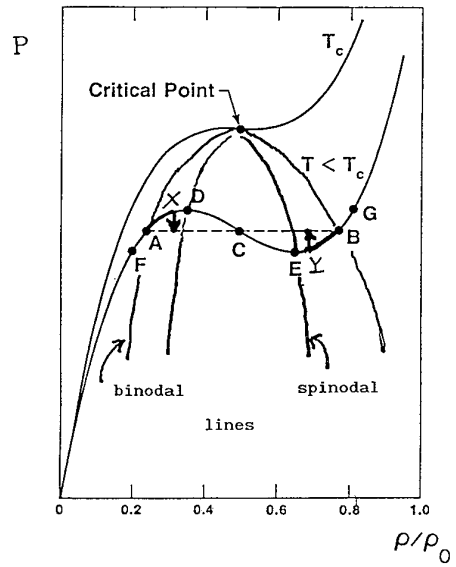


Fig. 2. The van der Waals isotherms calculated in the mean field approximation.

negative values for increasing $n$. In this case, for a density fluctuation large enough to pass the $W_n^*$ threshold (see Fig. 3) the spontaneous condensation of vapor continues. At the same time, due to an analogous mechanism, bubbles of vapor appear in the metastable liquid (point $Y$ in Fig. 2). Again, for large enough density fluctuations spontaneous evaporation of liquid occurs until the liquid–vapor equilibrium is attained (see the Maxwell construction line, Fig. 2). The droplet and bubble metastable states have definite life times. Their values depend on the intrusion distance into the metastability region and may be measured using *e.g.* special Wilson or bubble type chambers [12]. The DE section of the van der Waals isotherm is located inside the instability (spinodal) region. For the macroscopic liquid–gas system, the critical point, which belongs to the spinodal region, is the only one accessible experimentally (Fig. 4). The line of the maximal temperature of the superheated liquid is measured with great accuracy and is used as a test of models predicting position of the spinodal line, the border between the metastable and unstable spinodal regions [12].

Sequential evaporation of particles by atomic nuclei ($E < 1$ MeV/nucleon) also proceeds through metastable states and is a stochastic process, although its mechanism is rather different. As the nuclear temperature rises, nucleons increasingly occupy the continuum unbound states and escape from the nucleus. For a very short while there appears here something like a "vapor" of nucleons surrounding a "liquid drop". Nucleon density of such a "liquid

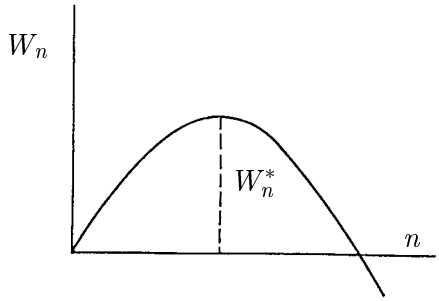


Fig. 3. Reversible work, $W$, of formation of a cluster containing $n$ molecules [11].

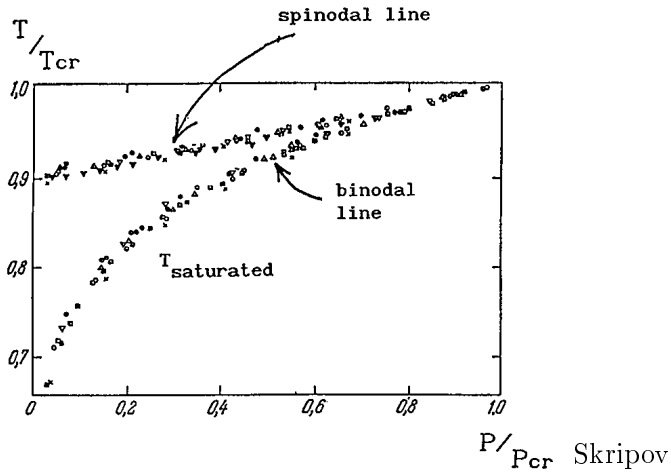


Fig. 4. Maximal temperatures $T_{\max}$ of different superheated liquids (the spinodal line) and temperatures $T$ of saturated vapors (the binodal line) [12].

drop" is close to the saturation density, $\rho_0$, of cold nuclear matter. One may speak in this case of a latent heat, related to the particle separation energy, and certainly $S$("liquid drop") $< S$("vapor"). However, the liquid-gas phase equilibrium does not exist here. The nuclear particle evaporation resembles rather the evaporation into vacuum of a macroscopic liquid.

## 2. Nuclear caloric curve

At higher excitation energies the measurement of the nuclear temperature is a difficult task. It may be done in several different ways [13], and I shall not discuss that subject here. The dependence of the nuclear temperature on the excitation energy, the so-called caloric curve, has been measured [14] and is the subject of heated discussions. The caloric curve obtained for

the $^{197}$Au+$^{197}$Au system at 600 MeV/u, together with the $^{12}$C,$^{18}$O+$^{nat}$Ag, $^{197}$Au at 30–84 MeV/u, and $^{22}$Ne+$^{181}$Ta at 8 MeV/u data is presented in Fig. 5. The He Li thermometer [15] was used here.

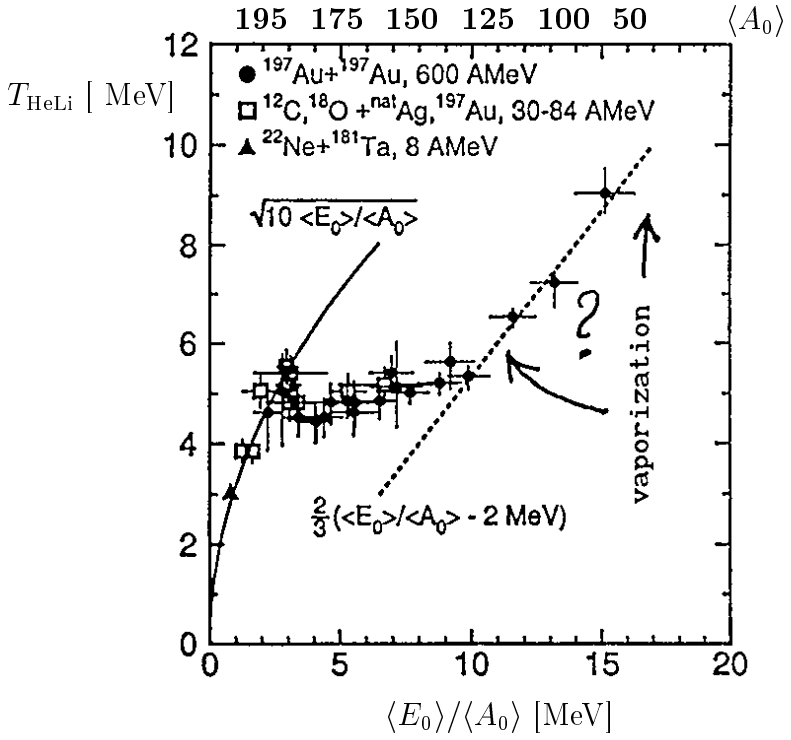


Fig. 5. The nuclear caloric curve [15].

In the Au+Au reaction properties of projectile-like fragments (gold like) were studied. For the others, the properties of composite systems formed by incomplete fusion were investigated.

Three different regions may be noticed in this caloric curve. For low excitation energies, smaller than about 2 MeV/u, the temperature varies in agreement with formula (4), with the density of state parameter $a = A/10$ MeV$^{-1}$. One can speak here of warming up a liquid drop of nuclear matter. For high energies, larger than about 10 MeV/u, the caloric curve resembles heating up an ideal gas. Here the temperature increases as the $2/3(E/A - 2\,\mathrm{MeV})$ function. In that region of excitation energies, one observes a growing vaporization of nuclei. The most intriguing is the intermediate region of the caloric curve, between 2 and 10 MeV/u. In fact this corresponds to the previously known limiting temperature line [16]. The lim-

iting temperature, the maximum temperature accessible for stable nuclei, is smaller than the critical temperature. It decreases with the nucleus mass, which may be noticed in the caloric curve of Fig. 5, where, due to the prequilibrium emission of particles in the early reaction stage, the observed mass of hot nuclei decreases with the excitation energy (see the average mass scale in the upper part of Fig. 5). As the temperature does not change too much in this excitation energy region, some have interpreted the corresponding part of the caloric curve as nuclear boiling [17], which has met with strong criticism [18].

Is it possible to find in the caloric curve some indication of a phase transition of the first kind? Before trying to answer this question I would like to attract your attention to some experimental facts.

There is experimental evidence indicating that at a high enough excitation energy, the sequential emission (SE) of particles is replaced by prompt multifragmentation (PM). It seems that one is observing here a Coulomb explosion of a set of fragments contained inside some volume, called the freeze-out volume. The freeze-out volume is, according to definition, the smallest volume, usually a sphere, in which constituents of the breaking up nucleus do not interact via nuclear forces. The Coulomb explosion time scale is expected to be definitely shorter than the sequential emission time scale.

The experimental search for differences between SE and PM is usually based on particle–particle correlations measured at small relative angles [19]. The relative velocity, $v_{\rm rel}$, of observed fragments is influenced after emission by the Coulomb repulsion, diminishing the number of particle–particle coincidences at small relative velocity. The degree of this effect (the size of the so called "Coulomb hole") is larger when the decay time is shorter. It may be observed in the correlation function, $R$, for pairs of fragments having charges $Z_i$ and $Z_j$, respectively:

$$1 + R = \frac{N_{ij}^{\rm true}(v_{\rm red})}{N_{ij}^{\rm mix}(v_{\rm red})}\,, \tag{6}$$

where the reduced velocity of fragments, $v_{\rm red} = v_{\rm rel}/(Z_i + Z_j)^{1/2}$, $N_{ij}^{\rm true}$ denotes the number of measured coincidences, and $N_{ij}^{\rm mix}$ the number of artificially produced random coincidences.

As an example, Fig. 6(a) presents the $R$ correlation function measured for hot Ca-like nuclei produced in the $^{40}$Ca+$^{40}$Ca reaction at 35 MeV/u [20]. The broken and solid lines represent here predictions of the SE and PM decay scenarios, respectively. As one can see, the SE scenario explains the experimental data at low excitations only, below about 3 MeV/u. At higher excitations one has to use a correlation function calculated according to the PM scenario. At the lowest excitation energy the average lifetime,

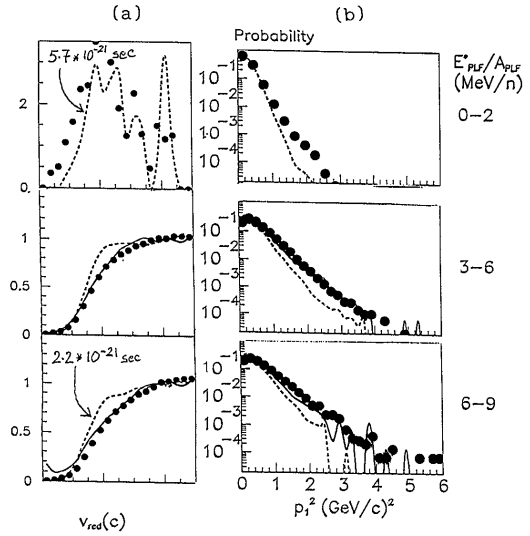


Fig. 6. $R$ correlation functions of particles emitted from hot projectile-like fragments, produced in the $^{40}$Ca+$^{40}$Ca reaction at 35 MeV/u (a), and corresponding distributions of $p_1^2$ (b), taken from [20].

$\tau$, of the excited Ca-like nucleus decaying by sequential emission is about 5.7 $10^{-21}$ sec. At the highest excitation energy, the $\tau$ characteristic of the sequential decay drops down to about 2.2 $10^{-21}$ sec, which is not enough to match the measured size of the "Coulomb hole". On the other hand the prompt decay of the hot system from the freeze- out volume gives the proper size of the "Coulomb hole".

Beside the $R$ correlation function one can apply two different signatures of prompt multifragmentation, which make use of different features of the decay from the freeze-out volume. These are: *(i)* the shape of the distribution of squared momentum, $p_1^2$, of the heaviest fragment emitted from the hot source, and *(ii)* the focusing of fragments of the hot source by the Coulomb field. It has been shown that the mean square momentum of the residue is always smaller than the mean of the sum of the squares of the momenta of sequentially emitted particles [21]. The situation is different for prompt multifragmentation, where a collective Coulomb "kick" received by the heaviest fragment from other particles of the freeze-out volume leads to the increase of the recoil momentum [22]. Fig. 6(b) displays the measured distribution of $p_1^2$ for different bins of the excitation energy of the hot Ca-like nucleus. The distributions are distinctly broader for energies higher than 3 MeV/u, in agreement with the PM decay scenario, and suggest the sequental emission of particles only below 3 MeV/u [20].

The Coulomb focusing effect is observed in the distribution of intermediate mass fragments, IMFs, displayed in a reference frame defined by the relative velocity of the two heaviest fragments [23]. The two heaviest fragments generate a Coulomb field strong enough to focus the velocities of IMFs around a 90-degree angle. This can be seen (Fig. 7) for a hot system ($\langle A \rangle \approx 70$) produced in the incomplete fusion of the $^{40}$Ca+$^{40}$Ca reaction at 35 MeV/u, and excited to an energy $\langle E/u \rangle \approx 7$ MeV/u [20]. For the sequential decay the distribution is distinctly flatter. In Fig. 7 we also see the $R$ and $p_1^2$ distributions. All three signatures indicate prompt multifragmentation from the freeze-out volume.

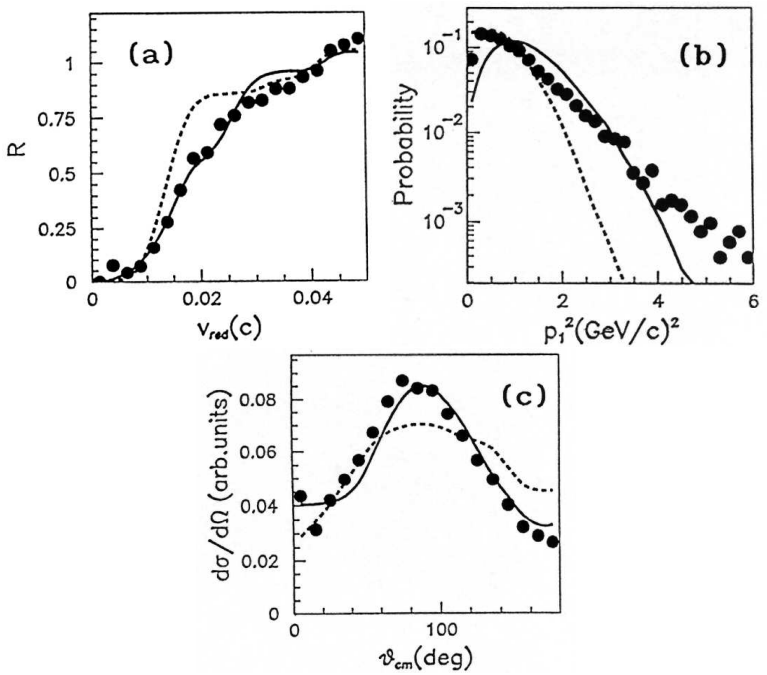


Fig. 7. $R$ correlation function (a), $p_1^2$ distribution (b), and IMF angular distribution measured in the reference frame defined by the relative velocity of the two heaviest fragments (c), for the hot system ($\langle A \rangle \approx 70$), produced in the incomplete fusion of the $^{40}$Ca+$^{40}$Ca reaction at 35 MeV/u [20].

What is the mechanism leading a nuclear system towards the freeze-out configuration? A different type of microscopic calculations [24], based on semi-classical kinetic equations with the collision term of Uehling and Uhlenbeck [25] and long range interactions included in the way proposed by Landau and Vlasov [26], suggests that in the dynamic process of a heavy ion collision, a hot and compressed nuclear system is created, which after-

wards expands and cools down. This process is accompanied by density fluctuations and depends on the final density $\rho$ of the hot nuclear system (see Bondorf *et al.* [27] and references cited therein). At $\rho_0/2 < \rho < \rho_0$ the "bubble phase" (with nucleon gas inside) is energetically more preferable, while at $\rho < \rho_0/2$ the phase of droplets surrounded by nucleons is realized. One is tempted to say that for a very short time we have here vapor–liquid equilibrium. This picture resembles the first order phase transition of the macroscopic fluid described in the preceding section as condensation or evaporation. In principle it can also be a spinodal decomposition, which here is also the first order phase transition (see Fig. 2).

Unfortunately there is evidence of a different kind that seems to contradict the above conclusion.

### 3. Validity of the mean field description — critical phenomena

For macroscopic matter as well as for nuclear, the equation of state is based on the mean field approximation. This approach fails at some distance from the critical point, where fluctuations grow together with their correlation length [28]. Let us look at the shape of the macroscopic liquid–vapor coexistence line for $t \to 0$ (Fig. 8). Here $t = (T - T_{\rm cr})/T_{\rm cr}$ ($T_{\rm cr}$ is the critical temperature). In the vicinity of the critical point the coexistence line may be approximated by:

$$\rho_{\rm liq} - \rho_{\rm vap} \sim |t|^{\beta} . \tag{7}$$

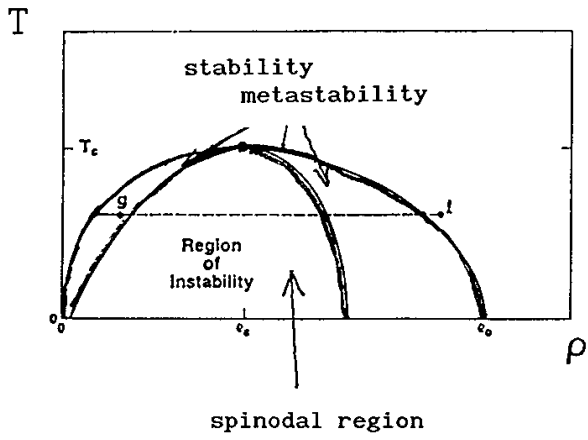


Fig. 8. The coexistence curve (solid line), and the spinodal curve (broken line) of a macroscopic liquid–vapor system.

For the mean field approximation $\beta = 1/2$, which means that for $t \to 0$ we have got a parabola. Measurements performed for two very different substances, xenon and sulphur hexafluoride in the range $3 \cdot 10^{-2} < t < 3 \cdot 10^{-6}$, show that one should use here $\beta = 0.32$ [29] and not $\beta = 1/2$. Similarly: the heat capacity

$$C_V = -T \left( \frac{\partial^2 F}{\partial T^2} \right) , \tag{8}$$

where $F = E - TS$ denotes the Helmholtz free energy, and the isothermal compressibility

$$K_T = \frac{1}{V} \frac{\partial V}{\partial p} . \tag{9}$$

For $t \to 0$ one can write:

$$C_V \sim |t|^{-\alpha} , \tag{10}$$

and

$$K_T \sim |t|^{-\gamma} . \tag{11}$$

In the mean field approximation $C_V$ has a jump at $t = 0$ (see Fig. 9) and $\gamma = 1.0$. However, the experiment suggests here $\alpha = 1/8$–$1/9$ and $\gamma = 1.23$, respectively [28, 30].

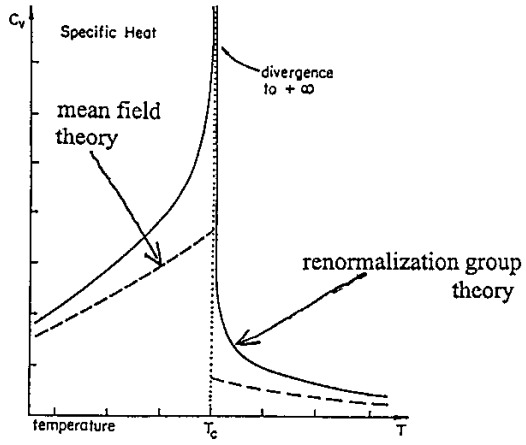


Fig. 9. Variation of the specific heat through the liquid–gas critical point [28].

The coefficients: $\alpha$, $\beta$, $\gamma$, and several others not mentioned here, are called the critical indexes (critical exponents). In the vicinity of the critical point the mean field approximation fails to reproduce their correct values, and one has to apply here some more sophisticated theoretical tools, such as the scaling models or the renormalization group theory [28].

## 4. How to study critical phenomena for atomic nuclei

It was suggested by Campi in 1986 [31] that, by analogy to large percolation lattices, one may study here moments of charge distributions of multifragmenting hot nuclear systems. For that purpose one has to measure, event by event, for a given multiplicity, $m$, of charged particles the numbers of fragments, $n_Z(m)$, having an electric charge $Z$. Now the charge moment of the order $k$ can be defined:

$$M_k(m) = \sum_Z Z^k n_Z(m) - (Z_{\max})^k \,. \tag{12}$$

Here $Z_{\max}$ corresponds to the largest "cluster" representing the "bulk liquid". For a certain critical multiplicity, $m_{\rm cr}$, one can now expect critical behavior. For instance:

$$M_0 \sim |m - m_{\rm cr}|^{2-\alpha} \,, \tag{13}$$

$$M_1 \sim (m - m_{\rm cr})^{\beta} \,, \qquad m \geq m_{\rm cr} \tag{14}$$

$$M_2 \sim |m - m_{\rm cr}|^{-\gamma} \,. \tag{15}$$

At the critical point, $m = m_{\rm cr}$, the distribution of the fragment charge should obey the power law:

$$n_Z(m) \sim Z^{-\tau} \,. \tag{16}$$

The critical indexes are not all independent, since *e.g.*:

$$\tau = 2 + \frac{\beta}{\beta + \gamma} \,. \tag{17}$$

Owing to the universality of the critical phenomena, the values of $\alpha$, $\beta$, $\gamma$ and $\tau$ measured here for the nuclear system should be the same as for the macroscopic liquid–vapor system, because both systems belong to the same universality class. Of course, due to the finite size of hot nuclei, $M_2$ shows a maximum for $m = m_{\rm cr}$ instead of a singularity.

Table I presents the values of $\beta$, $\gamma$, and $\tau$ measured in the Au+C reaction (Gilkes *et al.* [32], the EOS Collaboration) and in the $^3$He+Au reaction (Brzychczyk *et al.* [33]).

## 5. Problems

As can be seen in Table I, the critical indexes measured for hot nuclei have values close to those obtained for the macroscopic liquid–vapor system and are different from the predictions of the mean field calculations. It should be

TABLE I

Values of $\beta$, $\gamma$, and $\tau$, measured for the nuclear and macroscopic systems. $E/u$ and $T$ denotes the evaluated excitation energy and temperature, respectively.

| | $E/u$ (MeV) | $T$ (MeV) | $\beta$ | $\gamma$ | $\tau$ |
|---|---|---|---|---|---|
| Experiment: | | | | | |
| Au+C | 5.0 | 4.7 | $0.29 \pm 0.02$ | $1.4 \pm 0.1$ | $2.14 \pm 0.06$ |
| $^3$He+Au | 5.5 | 6.0 | | | $2.17 \pm 0.07$ |
| Macroscopic liquid-gas system | | | | | |
| Experiment: | | | 0.32 | 1.23 | 2.21 |
| Mean field calculation: | | | 0.5 | 1.0 | 2.33 |

noticed that for all three critical indexes the "mean field" values are located outside the range delimited by the "nuclear" and "macroscopic liquid–vapor". But hot systems produced in the Au+C and $^3$He+Au reactions lie on the caloric curve (see Fig. 5) which, as we know, is identical with the maximum temperature line, $T_{\max} = 4.5$–6 MeV. This temperature is much lower than the critical temperature calculated for hot nuclei, $T_{\rm cr} \approx 8$ MeV [34]. It has been argued that $T_{\max}$ is smaller than $T_{\rm cr}$ because of the long range Coulomb interaction, and should be called the crack temperature. However, this does not explain the critical phenomena observed in the vicinity of $T_{\max}$.

It has been suggested recently that the maximum heat capacity has been found in the Au+Au collisions at 35 MeV/u [35], which could be direct evidence for the second order phase transition. This result is based on calculations [36] indicating the existence of large fluctuations along the caloric curve. Temperatures and temperature fluctuations inside the freeze-out volume were obtained from the energies and masses of the contained particles. The authors suggest a phase transition in the region of the excitation energy of about 5 MeV/u and at the critical temperature 4–6 MeV, in disagreement with earlier calculations [34]. It is not clear why the second order phase transition takes place at the excitation energy of about 5 MeV/u and not in other places along the caloric curve which show similar multifragmentation properties, also indicate large $T$ fluctuations and belong to different mass nuclei (see [35] and comments on Fig. 5).

*Some more accurate measurements and new theoretical ideas are evidently necessary in order to solve these difficulties.* Then new $4\pi$ multidetector systems constructed at Texas A.& M. University, College Station, and at the Laboratorio Nazionale del Sud, Catania will be very useful.

It was suggested recently that the isospin degree of freedom may influence the values of the critical indexes and even more the value of the critical temperature [37]. The enrichment of the gas phase in neutrons, in comparison to the liquid phase (bound fragments), in the coexistence freeze-out volume seems to support this conjecture [38].

It would be interesting to check the vicinity of the eventual critical point using *the Ginzburg criterion* [39] known in condensed matter physics. According to this criterion there exists a finite region in the space of thermodynamic variables where, due to fluctuations, the mean field approximation does not work, and where critical phenomena may appear. How large is this region in the nuclear case, and does it correspond to the region where we suspect the existence of critical phenomena?

This work was supported by the Committee of Scientific Research of Poland (KBN Grant No 2P03B13941) and by the M. Skłodowska-Curie Fund (MEN/DOE-97-318).

## REFERENCES

[1] H. Feshbach, *Physics Today*, November 1987.

[2] see *e.g.* L. Landau, E. Lifszic, *Statistical Physics*, 1959.

[3] E. Erba *et al.*, *Nuovo Cim.* **22**, 1237 (1961).

[4] R. Stokstad, *The Use of the Statistical Model in Heavy-Ion Reaction Studies*, ed. D. Allan Bromley, Plenum Publishing, New York 1981.

[5] G. La Rana *et al.*, *Nucl. Phys.* **A488**, 211c (1988).

[6] N. Bohr, *Nature* **137**, 344 (1936).

[7] V.F. Weisskopf, *Phys. Rev.* 52 (1937).

[8] A.S. Botvina, D.H.E. Gross, *Phys. Lett.* **B344**, 6 (1995).

[9] B. Borderie, *Ann. Phys.* (Paris) **17**, 349 (1992); *Proc. of the Int. Conf. on Large Scale Collective Motion of Atomic Nuclei*, Eds. G. Giardina, G. Fazio, M. Lattuada, World Scientific, 1997, p. 1.

[10] D.H.E. Gross, *Rep. Prog. Phys.* **53**, 605 (1990).

[11] *Nucleation Phenomena* ed. A.C. Zettlemoyer, Elsevier Scientific Publishing Company, 1977.

[12] W.P. Skripov, *Metastable fluid*, Izdatielstvo NAUKA, Moscow 1972.

[13] see *e.g.* F. Gulminelli, D. Durand, *Nucl. Phys.* **A615**, 117 (1997); A.Siwek *et al.*, *Phys. Rev.* C57 (1998) 2507.

[14] J. Pochodzalla *et al.*, *Phys. Rev. Lett.* **75**, 1040 (1995); M.J. Huang *et al.*, MSU preprint MSUCL-1046 (1996); V. Serfling, PhD-thesis, Univ. Frankfurt a.M. (1997).

[15] S. Albergo *et al. Nuovo Cim.* **89A**, 1 (1985).

[16] see J.B. Natowitz *et al.*, *Phys. Rev.* **C52**, R2322 (1995), and references cited therein.

[17] see *e.g.* J. Pochodzalla, *Acta Phys. Pol.* **B28**, 357 (1997).

[18] L.G. Moretto *et al.*, LBL preprint LBNL-41273/UC-413 (1997); *Phys. Rev. Lett.* **76**, 2822 (1996).

[19] R. Trockel *et al.*, *Phys. Rev. Lett.* **59**, 2844 (1987).

[20] W. Gawlikowicz *et al.*, Institute of Physics, Jagellonian University preprint ZFGM-99-02 (1999).

[21] A.J. Cole *et al.*, *Nucl. Phys.* **A583**, 537 (1995).

[22] K. Grotowski, *Acta Phys. Pol.* **B24**, 285 (1993).

[23] W. Gawlikowicz, K. Grotowski, *Nucl. Phys.* **A551**, 73 (1991).

[24] J. Aichelin *et al.*, *Phys. Rev.* **C31**, 22 (1985); H. Kruse *et al.*, *Phys. Rev.* **C31**, 1770 (1985); C. Gregoire *et al.*, *Nucl. Phys.* **A465**, 317 (1987).

[25] E.A. Uehling, G.E. Uhlenbeck, *Phys. Rev.* **43**, 552 (1993).

[26] R. Balescu, *Equilibrium and Nonequilibrium Statistical Mechanics*, Wiley, New York 1975.

[27] see Bondorf *et al.*, *Phys. Rep.* **257**, 133 (1995), and references cited herein.

[28] M.E. Fischer, *Advanced Course on Critical Phenomena*, The Merensky Institute of Physics University of Stellenbosch, South Africa, 1982.

[29] D. Balzarini, K. Ohrn, *Phys. Rev. Lett.* **29**, 840 (1972); *Can. J. Phys.* **52**, 499 (1974).

[30] M.I. Bagatskii *et al.*, *Sov. Phys. JETP* **16**, 517 (1963).

[31] X. Campi,*Phys. Lett.* **B208**, 351 (1988).

[32] M.L. Gilkes *et al.*, *Phys. Rev. Lett.* **73**, 1590 (1994).

[33] J. Brzychczyk *et al.*, *Phys. Rev.* **C58**, R1372 (1998).

[34] L. Satapathy *et al.*, *Phys. Rev.* **C39**, 62 (1989).

[35] M. D'Agostino *et al.*, *Nucl. Phys.* **A650**, 327 (1999).

[36] Ph. Chomaz, F. Gulminelli, *Nucl. Phys.* **A647**, 153 (1999).

[37] Ph. Chomaz, F. Gulminelli, *Phys. Lett.* **B447**, 221 (1999); H. Müller, B.D. Serot, *Phys. Rev.* **C52**, 2072 (1995).

[38] H.S. Xu *et al.*, Michigan State University preprint MSUCL-1137 (1999).

[39] V.L. Ginzburg, *Sov. Phys.* **2**, 1824 (1960); J. Als-Nielsen, R.J. Birgeneau, *Am. J. Phys.* **45**, 554 (1997).